

Computer simulation of operation plant effective modes for water disinfection by electrical discharges in gas bubbles

Purpose. Determination by means of computer simulation of the most efficient modes of operation of the installation for water disinfection using discharges in gas bubbles, in which (modes) the amplitude of voltage pulses at the processing unit and on the layer of treated water is not less than the voltage amplitude immediately after the switching discharger. **Methodology.** To achieve this goal, we used computer simulation using Micro-Cap 10. We used two different electrical circuits that simulate the operation of the experimental setup in two different modes: in a mode with a restoring electrical strength of the discharge gap in the gas bubble between two adjacent voltage pulses on the discharge node and in the mode without restoring this dielectric strength. In computer simulation, we varied the following factors: the maximum simulation step, inductances, capacitances, active resistances, wave resistance of a long line, and the delay time for the operation of a spark gap simulating a discharge gap in a gas bubble. **Results.** Computer modeling has shown that in order to increase the voltage amplitude at the treatment unit and on the layer of treated water, it is necessary to reduce the load capacitance – the capacitance of the water layer in the treatment unit to 10 pF or less, to increase the active resistance of the water layer to 500 Ω or more. An important factor for increasing the voltage and electric field strength in the discharge unit and, consequently, for increasing the efficiency of treated water disinfection is the discharge delay time in gas bubbles. The most rational delay time for the operation of the arrester, which is the gap in the gas bubble inside the water, under the conditions considered by us is 4–5 ns. It is with this delay time that the amplitude of voltage pulses at the node of disinfecting water treatment and on the layer of treated water is maximum, all other things being equal. Furthermore, with such a delay time this amplitude of voltage pulses significantly exceeds the voltage amplitude directly after the main high-voltage discharger, switching energy from the high-voltage capacitive storage to the processing unit through a long line filled with water. **Originality.** Using computer simulation, we have shown the possibility of increasing the voltage at the discharge unit of the experimental setup by 35 % without increasing the voltage of the power source. This provides a higher efficiency of microbiological disinfection of water by nanosecond discharges in gas bubbles and lower specific energy consumption. **Practical value.** The obtained results of computer simulation confirm the prospect of industrial application of installations using nanosecond discharges for disinfection and purification of wastewater, swimming pools and post-treatment of tap water. References 15, figures 10.

Key words: high-voltage water disinfection unit, discharge unit, sharpening spark gap, discharge in gas bubbles in water, discharge delay time, long electric line.

Мета. Визначення за допомогою комп'ютерного моделювання найбільш ефективних режимів роботи установки для знезараження води за допомогою розрядів у газових бульбашках, при яких (режимах) амплітуда імпульсів напруги на вузлі обробки та на шарі води, що обробляється, не менше амплітуди напруги безпосередньо після комутуючого розрядника. **Методика.** Для досягнення поставленої мети ми використовували комп'ютерне моделювання за допомогою Micro-Cap 10. Ми використовували дві різні електричні схеми, що моделюють роботу експериментальної установки в двох різних режимах: в режимі з електричною міцністю, що відновлюється, розрядного проміжку в газовій бульбашці між двома сусідніми імпульсами напруги на розрядному вузлі та у режимі без відновлення цієї електричної міцності. При комп'ютерному моделюванні варіювалися такі фактори: максимальний крок при моделюванні, індуктивності, ємності, активні опори, хвильовий опір довгої лінії, час затримки спрацьовування розрядника, що моделює розрядний проміжок у газовому міхурі. **Результати.** Комп'ютерне моделювання показало, що для збільшення амплітуди напруги на вузлі обробки і на шарі води, що обробляється, слід зменшувати навантажувальну ємність – ємність шару води у вузлі обробки до 10 пФ і менше, збільшувати активний опір шару води до 500 Ом і більше. Важливим чинником збільшення напруги і напруженості електричного поля в розрядному вузлі і, отже, збільшення ефективності знезараження оброблюваної води є час затримки розряду в газових бульбашках. Найбільш раціональний час затримки спрацьовування розрядника, яким є зазор у газовій бульбашці всередині води, у розглянутих умовах становить 4-5 нс. Саме при такому часі затримки амплітуда імпульсів напруги на вузлі знезаражувальної обробки води і на шарі оброблюваної води є максимальною за інших рівних умов і істотно перевищує амплітуду напруги безпосередньо після основного високовольтного розрядника, що комутує енергію з високовольтного ємнісного нагромаджувача у вузол обробки. **Наукова новизна.** За допомогою комп'ютерного моделювання показана можливість підвищення напруги на розрядному вузлі експериментальної установки на 35 % без збільшення напруги джерела живлення, що забезпечує більш ефективне мікробіологічне знезараження води за допомогою наносекундних розрядів у газових бульбашках за малих питомих витрат енергії. **Практична значущість.** Отримані результати комп'ютерного моделювання підтверджують перспективу промислового застосування установок з використанням наносекундних розрядів для знезараження та очищення стічних вод, басейнів та доочищення водопровідної води. Бібл. 15, рис. 10.

Ключові слова: високовольтна установка для знезараження води, розрядний вузол, розрядник, що загострює, розряд у газових бульбашках у воді, час запізнення розряду, довга електрична лінія.

Introduction. In recent years, various scientists have carried out intensive researches of the characteristics and considered prospects for the technological use of nanosecond discharges in gas bubbles inside liquids in various high-voltage installations [1–3]. These studies use both experimental methods and computer simulations. The latter is widely used in various fields of electrical engineering [4, 5].

Authors of [6] have shown microbubbles are very fine bubbles that shrink and collapse underwater within several minutes, leading to the generation of free radicals.

The characteristics of a multiple argon bubble jet in which a streamer is generated by a dc pulsed discharge have been experimentally clarified through discharge

visualization in a bubble and decolorization of a methylene blue solution [7].

In [8] authors have investigated experimentally a water treatment, which introduces a vaporized solution into a coaxial dielectric barrier discharge tube using Ar.

Authors of [9] provided a concise review of the state-of-art for research on plasma-bubble interactions and a perspective for future research.

The objective of the thesis [10] was to utilize plasma discharges to treat a large volume of produced water for recycling it for subsequent fracking. To recycle produced water, both bacterial inactivation and water softening are required, which are the two main objectives of the present study of plasma water treatment.

Authors of [11] achieved the next results. The discharge propagates into the bubble from the tip of the wire in the glass tube. Then, the discharge propagates along the bubble surface. The propagation velocity is almost independent of water conductivity and is $(2.7-3.6) \cdot 10^5$ m/s. The average maximum length of the discharge propagation decreases from approximately 8.9 to 5.4 mm with increasing water conductivity from 7 to 1000 $\mu\text{S/cm}$. Indigo carmine, a commonly used organic dye, was used as the chemical probe of the active species produced by the discharge inside the bubble. The amounts of indigo carmine decomposition with 120 min of treatment is 0.24–0.26 μmol and independent of water conductivity. Meanwhile, the energy efficiency for the indigo carmine decomposition in water decreases from 18 to 7.3 $\mu\text{mol/Wh}$ with increasing water conductivity from 7 to 1000 $\mu\text{S/cm}$. The amount of hydrogen peroxide production by the treatment increases from 2.0 to 3.1 μmol with increasing the conductivity.

In article [12] authors start by describing our experimental methodology addressing bubble geometry and timing methods. For the first time, we present an original method of bubble positioning with control of statistical information of the bubble shape, size, and position between the electrodes. A unique timing scheme is introduced that allows the application of the voltage pulses when a bubble is in the desired position between the electrodes. Finally, the experimental results and discussion section present our evidence for the discharge initiation for two electrode configurations by order of timescale.

In our work [13], we have shown that when using nanosecond discharge pulses in gas bubbles, one should take into account the presence of long lines during the transmission of generated voltage pulses from sharpening spark gaps to units of water disinfection treatment. At the same time, we indicated that for all considered processing modes, the voltage amplitude at the processing nodes (at the output of a long line) is less than after the sharpening spark gap at the input of a long line. The question arises: are there modes in which the voltage amplitude at the nodes (node) of processing (load) is greater than at the input to long lines?

It is very important to answer the question of the possibility of obtaining the amplitudes of nanosecond voltage pulses directly on the load greater than the amplitudes of voltage pulses obtained because of switching the sharpening spark gap immediately after it. The load is a serial connection of a gas bubble with a discharge inside it and a layer of water. The magnitude of the voltage amplitude of these pulses determines the efficiency of the production of active particles and radiation in the node (or nodes) of water treatment and, consequently, the efficiency of disinfecting water treatment. Experimentally, using direct measurements of voltage pulses at the processing unit is extremely difficult. Therefore, we use the computer simulation method for this.

In this work, we consider the following two modes of operation of the installation. The first mode is one in which the electric strength of the gas in the bubble is restored after each discharge. The second regime is one in which the electric strength of the gas in the bubble is not restored after each discharge, i.e. the plasma channel(s) burns (burn) continuously. Let us also consider the effect on the voltage amplitude at the processing node of the discharge delay time in the gas bubble of the node, as well as the effect of the inductance, capacitance and active resistance of the processing node on the amplitude of this voltage, all other things being equal.

An increase in the amplitude of nanosecond voltage pulses at the processing unit (a series connection of a gas bubble with a discharge and a water layer) at a given voltage amplitude at the input of a long line filled with water and located in front of the discharge unit is an important task. Such an increase in amplitude makes it possible to increase the production of active particles in the processing unit and the intensity of broadband radiation from plasma channels.

The **purpose** of the work is to determine, using computer simulation, the most efficient modes of operation of the installation for water disinfection using discharges in gas bubbles, in which (modes) the amplitude of voltage pulses at the processing unit and on the layer of treated water is not less than the voltage amplitude immediately after the switching spark gap.

Electrical circuits for computer simulation and the influence of the maximum step size in computer simulation. A diagram with a discharge gap in a gas bubble that restores its electrical strength after each discharge is shown in Fig. 1.

Figure 2 shows a diagram with a discharge gap in a gas bubble in which, once ignited, the discharge does not go out (with a discharge gap that does not restore its electrical strength after each discharge).

Figure 3 demonstrates a schematic drawing of three discharge units of the experimental setup is presented, in each of which an electric discharge occurs in gas bubbles [14].

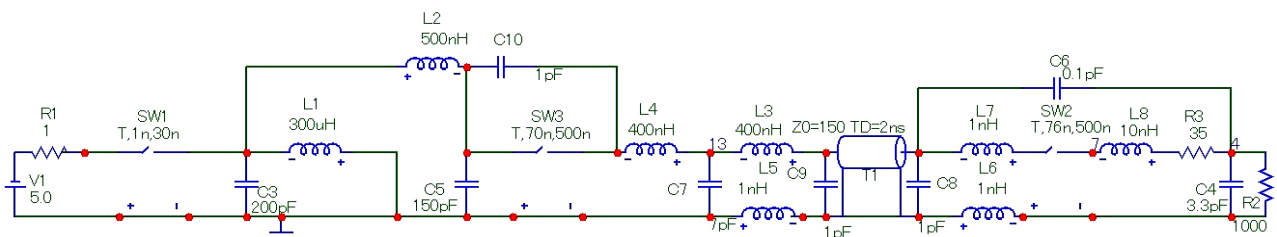


Fig. 1. Scheme with a discharge gap in a gas bubble, restoring its dielectric strength after each discharge

pipes is $d \approx 300$ mm. The flow rate of water and gas from the compressor is adjustable. The composition of the gas may be different. The flow of water can be carried out by gravity from a source of water 10.

Let us consider the influence on the results of computer simulation of the maximum step size in computer simulation, the delay time of operation of the terminal sharpening spark gap SW2, which is the gap in the gas bubble between the tip of the high-voltage electrode and the interface between the gas bubble and water. Besides let us consider the influence the capacitance C4 of the water layer and the operating modes of the spark gap SW2: with restoration of its electrical strength between two adjacent discharges and without such restoration of electrical strength.

We used two different steps for the simulation of the transient process: 0.2 ns and 0.01 ns.

Figure 5 shows the results when using the maximum step of 0.01 ns in a computer simulation. Figure 5

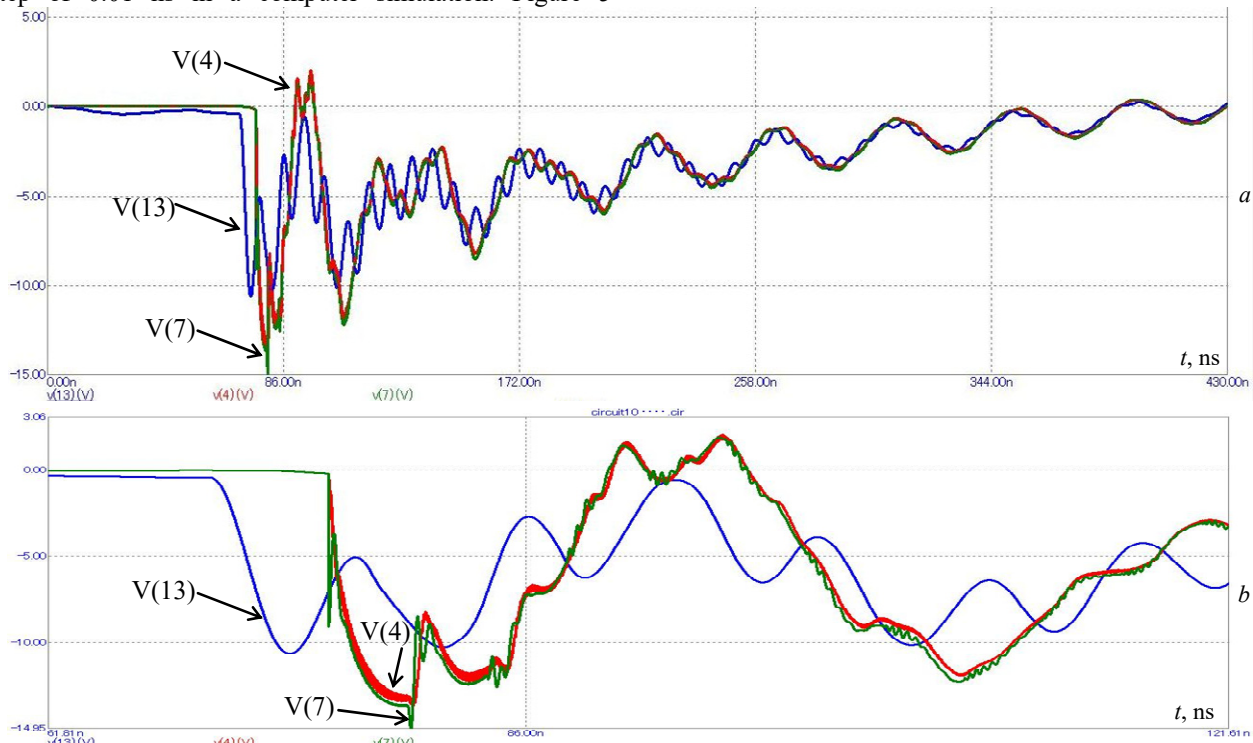


Fig. 5. Dependence of pulse voltages V(4), V(7), V(13) on time with a maximum simulation step of 0.01 ns: a – pulses in general; b – initial sections of these pulses ($T = 76$ ns, $R3 = 35 \Omega$, $C4 = 3.3$ pF, $Z0 = 150 \Omega$ – wave resistance, $L8 = 10$ nH, $R2 = 1000 \Omega$, $t_{step} = 0.01$ ns)

Under the conditions considered in this work, the main transient process occurs in the experimental setup in the first approximately 120 ns. Therefore, voltage pulses as a whole, with their characteristic duration up to 200–300 ns, are shown only in Fig. 5. It follows from simulation that the steepest parts of the model waveforms are better reproduced when using a finer maximum step of 0.01 ns. Therefore, we carried out further simulations in Micro-Cap 10 using a maximum step of 0.01 ns.

Influence of the discharge delay time in a gas bubble on the transient process in the discharge unit. We took into account that, at nanosecond fronts and pulse durations, the electrical strength of the discharge gaps increases significantly. Fig. 6 illustrates this circumstance.

Computer simulation makes it possible to check which voltage pulses are formed on the discharge node in the case when the electrical strength of the discharge gap has time to recover between two adjacent discharges, and

illustrates the results of simulation of voltage pulses V(4), V(7), V(13) as functions of time t according to the circuit in Fig. 1. This is under the following conditions: the moment T of the operation of the spark gap SW2 after the start of the transient process in the circuit $T = 76$ ns (the delay time of the operation of the spark gap SW2 after the arrival of the voltage wave front at the end of the long line TD is 4 ns). The long line TD is filled with water. Wherein, the final active resistance R3 of the discharge channels in gas bubble $R3 = 35 \Omega$, capacitance C4 of the water layer $C4 = 3.3$ pF, active resistance R2 of the water layer $R2 = 1000 \Omega$, inductance L8 of the discharge channels in the gas bubble $L8 = 10$ nH.

These are the parameters for the variant with one processing node. Voltages V(4), V(7), V(13) – voltages respectively between points 4, 7, 13 and the grounded point.

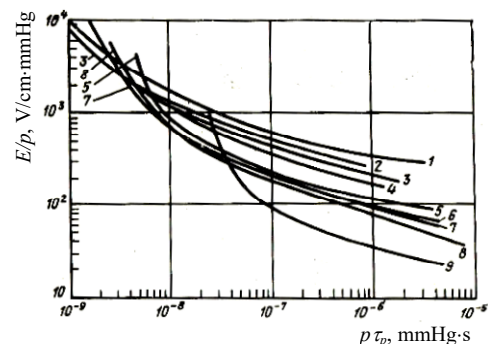


Fig. 6. [15, p. 22]. Dependence of E/p on $p\tau_p$ for various gases: 1-3 – freon of various grades; 4 – SF₆; 5 – O₂; 6 – air; 7 – N₂; 8 – Ar; 9 – Ne

also in the case when the electrical strength does not have time to recover, and the plasma channel (channels) burns (burn) continuously.

The discharge node is both a node for disinfecting treatment and water purification, on the one hand, and a source of all factors for such treatment, on the other hand.

Figure 7 (the delay time of the discharge in the gas bubble is not taken into account) and Figure 5 (the delay time of the discharge in the gas bubble is 4 ns) present the results of computer simulation of the influence of the delay time of the discharge in the gas bubble. We keep in mind the influence of the delay time of such discharge on

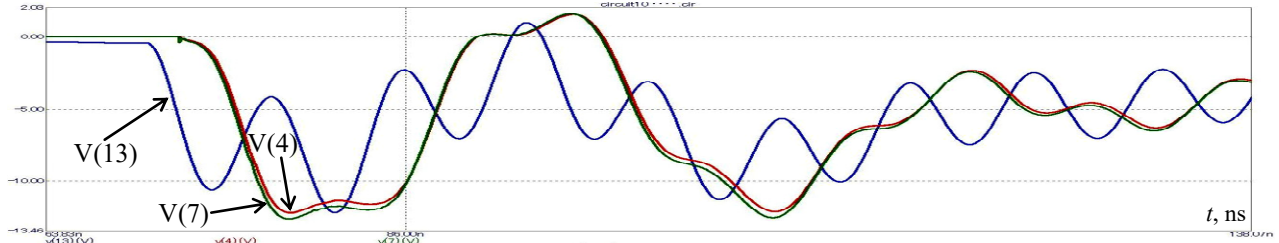


Fig. 7. Dependence of pulsed voltages V(4), V(7), V(13) on time without taking into account the delay time of the discharge in the gas bubble: initial sections of these pulses ($T = 72$ ns, other values – as for Fig. 5)

Let us estimate the capacitance C of the treated water layer as the capacitance of the flat capacitor with the effective square S of capacitor plates that is equal $S = 10^{-4}$ m² and the thickness d of water layer $d = 10^{-2}$ m:

$$C = \epsilon\epsilon_0 S/d = 81 \cdot 8.85 \cdot 10^{-12} \cdot 10^{-4}/10^{-2} \approx 6.9 \cdot 10^{-12} \text{ F.}$$

In [4], we did not take into account the delay time of the discharge in the discharge node of the disinfection treatment, i.e. it was assumed that the discharge in the gas bubble begins at the instant of arrival of the voltage pulse at the discharge unit after a long line (with an electrical length of 2 ns). The discharge delay time is the sum of the statistical delay time during which an effective electron appears in the discharge gap (effective electrons appear) and the discharge formation time.

Let us estimate the discharge formation time using the formula [15, p. 21]

$$\tau_p = [1/(\alpha v)] \ln[i_{cr} d / (e N_0 v)],$$

where τ_p is the discharge formation time; α is the impact ionization coefficient, which determines the number of electrons created by the primary electron when passing a distance of 1 cm in an electric field; v is the drift velocity of the electron avalanche; i_{cr} is the critical value of the current in the discharge circuit, which is reached by the current in the discharge circuit at the end of the discharge formation time; d is the length of the discharge gap; e is the electron charge; N_0 is the initial number of electrons (initiating electrons) that initiate the development of electron avalanches.

According to [15, p. 10] for air, the relation $\alpha/p = A(E/p - B)^2$ is valid, where $A = 1.17 \cdot 10^{-4}$ cm·mmHg/V², $B = 32.2$ V/(cm·mmHg). So $\alpha = A(E/p - B)^2 p$. In the nanosecond range of characteristic pulse durations, one can take $E = 100$ kV/cm = 10^5 V/cm. Then, at $p = 760$ mmHg $\alpha = A(E/p - B)^2 p = 1.17 \cdot 10^{-4} (10^5/760 - 32.2)^2 \cdot 760 \approx 878$ 1/cm.

In addition, according to [15, p. 20-21] it is possible to accept $v = 10^7$ cm/s, and at i_{cr} , which is much smaller than the current in the discharge circuit, the value $[i_{cr} d / (e N_0 v)] \sim 10^8$. From here we get $\ln[i_{cr} d / (e N_0 v)] \approx \ln 10^8 \approx 18.42$:

$$\tau_p = [1/(\alpha v)] \ln[i_{cr} d / (e N_0 v)] \approx [1/(878 \cdot 10^7)] \cdot 18.42 \approx 2 \cdot 10^{-9} \text{ s.}$$

Thus, the estimated calculated value of the discharge formation time was $\tau_p = 2 \cdot 10^{-9}$ s, i.e. 2 ns. The statistical

the amplitude of the voltage pulses at the discharge node (according to the scheme in Fig. 1).

Computer simulation in Micro-Cap 10 shows that there is the most rational time delay of the discharge in the gas bubble with respect to the moment. At this moment, the front of the falling voltage pulse arrives at the discharge unit with a gas bubble at the output of a long transmission line with water. This most rational time is approximately 4-5 ns.

delay time when voltage pulses with a steep edge (with a rise rate of $\geq 10^{12}$ V/s) are applied to the discharge gap does not exceed the value of the formation time.

To increase the voltage amplitude at the processing node and on the water layer in this node, it is necessary to reduce the load capacitance (capacity of the water layer in the processing node) to 10 pF or less, increase the active resistance of the water layer to 500 Ω or more.

It is important to estimate the ratio of the voltage across the entire discharge node (the voltage across the discharge channels in the gas bubble plus the voltage across the water layer) and the voltage directly across the water layer. The gap in the gas bubble between the tip of the high-voltage electrode and the interface with the water layer is the terminal sharpening gas discharger in the discharge channel(s) of which broadband radiation is formed and active micro-particles are formed that disinfect water.

Computer simulation showed that for the one shown in Fig. 1 of the circuit, close to the most rational delay time T for the operation of the spark gap SW2 relative to the moment of arrival of the front of the incident voltage wave along the long line is equal $T \approx 4$ ns. In this close to optimal mode, the spark gap SW3 operates 70 ns after the start of the transient process in the circuit in Fig. 1, and the arrester SW2 fires 76 ns after the start of this transient process. Taking into account the fact that between these arresters there is a long line T1 with an electrical length of 2 ns, from the moment 72 ns of the arrival of the front of the incident wave traveling along the long line T1, another 4 ns passes to the arrester SW2 until the moment of 76 ns of its operation. These four ns is the delay time operation of the spark gap SW2, close to most rational. With a smaller and longer delay time for the operation of the spark gap SW2, the voltage amplitude V(7) at the processing unit and at the water layer V(4) in the treatment unit decreases with a practically unchanged voltage amplitude V(13) immediately after the spark gap SW3. In a mode close to optimal (see Fig. 4), the voltage amplitude V(7) at the processing node exceeds the voltage amplitude V(13) by 1.35 times, and the source voltage V(1) is more than 2.7 times. At the same time, the voltage amplitude V(7) on the entire processing unit slightly

exceeds the voltage amplitude $V(4)$ on the water layer. This excess is the smaller, the lower the final resistance $R3$ of the plasma channels (because of discharges) in the gas bubble. Figure 5 illustrates the voltage versus time dependences at three different points in the circuit (see Fig. 1) for the case when we are considering one multi-gap spark gap $SW3$, one long line $T1$, and one water treatment unit. This unit comprises one discharge gap $SW2$, and is electrically connected in series with it a layer of water having a capacitance $C4 = 3.3$ pF and an active resistance $R2 = 1000$ Ω .

Voltage versus time for the case when three identical multi-gap spark gaps connected in parallel are used. Figure 8 illustrates the voltage versus time dependences at the same three points [$V(4)$, $V(7)$, $V(13)$] of the circuit (see Fig. 1), for which some results have already been discussed above, for the case when three identical multi-gap arresters connected in parallel in the experimental setup. In the diagram (Fig. 1), these arresters are represented as one resulting spark gap $SW3$, three identical long lines with an electrical length of 2 ns, connected in parallel, and are represented by the resulting long line $T1$ with a threefold reduced wave resistance $Z0 = 50$ Ω . In this case, three water treatment units are also used, each consisting of one discharge gap and a layer of water electrically connected to it in series. These three identical processing nodes

during modeling are combined into one node with the resulting discharge gap $SW2$ and the resulting water layer electrically connected to it in series, having a capacitance $C4 = 10$ pF and active resistance $R2 = 333$ Ω . At the same time, some other elements of the circuit have values that differ from those shown in Fig. 1, namely, $C8 = C9 = 3$ pF, $L6 = L7 = 0.33$ nH, $L8 = 3.3$ nH, $R3 = 12$ Ω . $L8$ and $R3$ are, respectively, the inductance and the calculated final active resistance of the resulting discharge gap $SW2$.

Both Fig. 5 and Fig. 8 show that the front of the pulses at points 4 and 7 is associated with the processes of reflection from the discharge gap $SW2$ at the end of the long line $T1$ and the path of voltage waves along the long line $T1$. The time interval between adjacent voltage surges caused by the reflection of voltage waves from the discharge gap $SW2$ is 4 ns, i.e. is equal to the double time of the wave travel along the line $T1$. On the oscillograms in Fig. 5, the voltage front for pulses $V(4)$ and $V(7)$ is much steeper than in Fig. 8, and is approximately 4 ns. In both of these figures, the voltage amplitude at the discharge nodes as a whole $V(7)$ and at the water layer $V(4)$ is greater than the voltage amplitude immediately after the multi-gap spark gap $SW3$. This was achieved by reducing the calculated capacitance of the water layer $C4$ to a value of 10 pF or less and choosing a delay time of 4 ns (close to optimal) for the operation of the spark gap $SW2$.

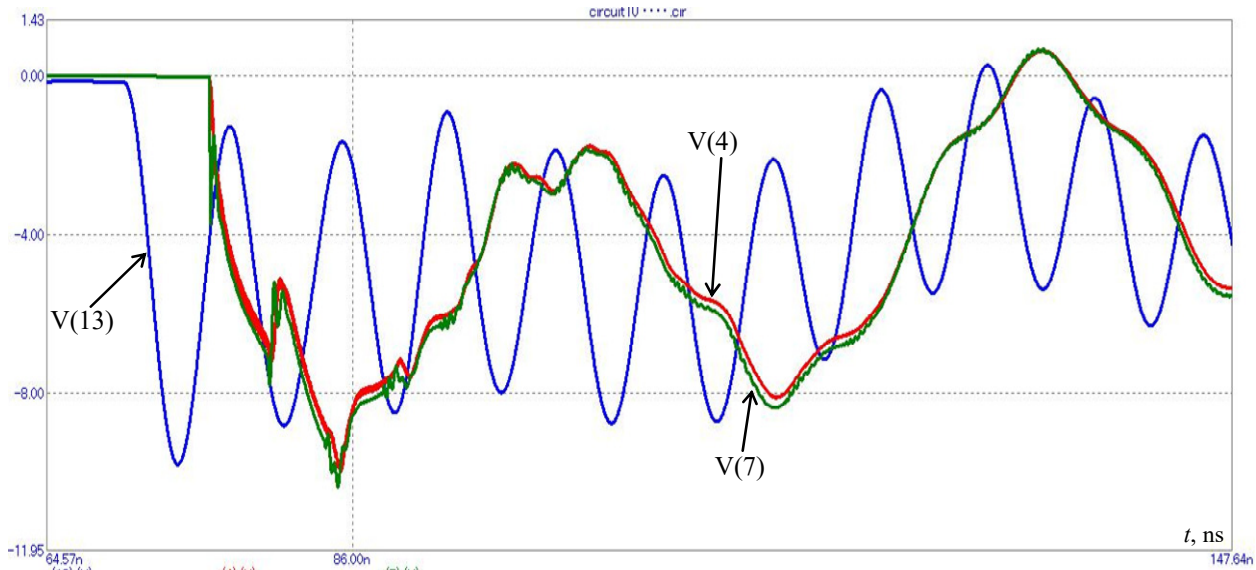


Fig. 8. Dependences of voltages $V(4)$, $V(7)$, $V(13)$ on time according to the diagram in Fig. 1 for the case with three processing units.

In this case three identical multi-gap spark gaps (their common designation $SW3$) connected in parallel are used:

initial sections these pulses ($T = 76$ ns, $R3 = 12$ Ω , $C4 = 10$ pF, $Z0 = 50$ Ω – wave resistance, $L8 = 3.3$ nH, $R2 = 333$ Ω , $t_{step} = 0.01$ ns)

The mode without taking into account the restoration of the electrical strength of the discharge gap in the gas bubble in comparison with the mode in which the electrical strength of the gap is restored. Figure 9 shows the results of computer simulation for the operating mode of the experimental setup, when the plasma channels after discharges do not disappear until the next high-voltage pulse arrives, that is, the electric strength of the gas gap in the gas bubble does not have time to recover between two voltage pulses adjacent in time. This mode corresponds to the operation of an experimental setup with one processing unit, in which the plasma channels in the gas bubble burn continuously, and

one sharpening multi-gap spark gap $SW3$, the electrical circuit of which is shown in Fig. 2. In this figure, the spark gap $SW2$ is absent, since the plasma channels (plasma channel) are well conducting, do not play the role of a switch, the impedance of which varies from a value much greater than the impedance of the discharge circuit to a value much less than the impedance of the discharge circuit. On Fig. 2 point number 7 in Fig. 1 has the number 12. As an estimate, we took both for the mode with the restoration of the electric strength of the discharge gap in the gas bubble, and for the mode without restoring its electric strength, when using one processing unit. The final (after the end of the transient) active resistance of the

plasma channels (plasma channel) $R3 = 35 \Omega$, inductance $L8 = 10 \text{ nH}$ (see Fig. 2) in both these modes.

Comparison of the results of simulation of the regime taking into account the restoration of the electrical strength of the discharge gap in the gas bubble after each discharge (the main mode) and the regime without taking into account the restoration of the electrical strength of this discharge gap (without the arrester SW2) shows the following. The presence of the spark gap SW2, considering the delay time of its operation, which is close to most rational, takes place in the main mode. The amplitude of voltage pulses, when taking into account the restoration of electric strength, is greater by about 20 % (see Fig. 5 and Fig. 9). The conditions for the reflection of a voltage wave, taking into account the delay time of operation SW2 and the restoration of the electric strength of the discharge gap in the gas bubble, are closer to the conditions reflections from the end of a long line (in our case, the T1 line) that is open at the end. In addition, in the regime without taking into account the restoration of the electrical strength of the discharge gap in the gas bubble after each discharge, the

curves of the voltage pulses $V(4)$, $V(12)$, $V(13)$ are very similar to each other with a somewhat lower amplitude of the voltage $V(4)$ on the layer water. A feature of the regime without taking into account the restoration of the electrical strength of the discharge gap in the gas bubble is that the plasma channels in the gas bubble burn continuously, providing broadband continuous radiation, including ultraviolet and even shorter wavelength. In this case, energy is supplied to the discharge unit by nanosecond pulses with a certain repetition rate. The energy supply to the discharge unit by nanosecond pulses is provided by a high-voltage capacitive storage with a capacity of $C5 = 150 \text{ pF}$ and a multi-gap spark gap SW3, the dielectric strength of which is restored much faster than that of SW2. The maximum repetition rate of pulses to the processing unit is determined by the minimum possible recovery time for the electrical strength of the spark gap SW3. If the pulse repetition rate exceeds the maximum, the electrical strength of the spark gap SW3 will not be restored, and the real experimental setup will go into emergency short circuit mode, which is unacceptable.

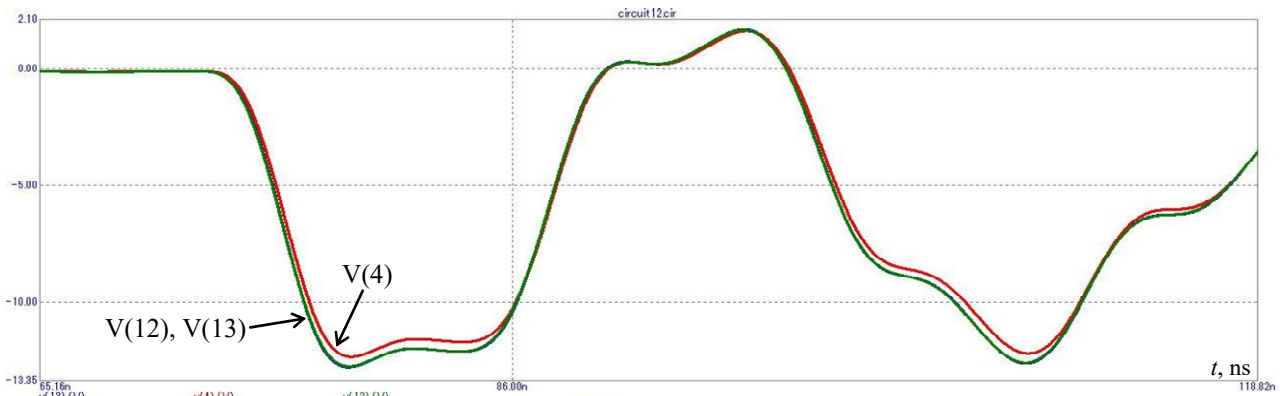


Fig. 9. Dependences of voltages $V(4)$, $V(12)$, $V(13)$ on time in the mode without taking into account the restoration of the electrical strength of the discharge gap in the gas bubble (according to the scheme in Fig. 2). This is the case with one processing unit: the initial sections of these pulses (the arrester SW2 is replaced by a segment of the conductor, so the parameter T is absent). The remaining values correspond to the values in Fig. 4)

Influence of the capacitance value of the water layer on the voltage amplitude at the processing unit. Figure 7 and Fig. 10 show that with an increase in the capacitance of the $C4$ water layer from $C4 = 3.3 \text{ pF}$ (Fig. 7) to $C4 = 50 \text{ pF}$ (Fig. 10) the voltage amplitude at the processing unit $V(7)$ and at the water layer $V(4)$ becomes significantly less than the voltage amplitude $V(13)$ after the spark gap SW3. In this case, the voltage amplitude $V(13)$

practically does not change. Our calculations show the next thing. When we are using an experimental setup, in order for the amplitude of the voltage pulses at the processing unit and on the water layer to be no less than the amplitude of the voltage pulses directly after the spark gap SW3, the capacitance of the water layer $C4$ should not exceed 20 pF . Figure 1 demonstrates the electrical circuit of this setup for computer simulation in Micro-Cap 10.

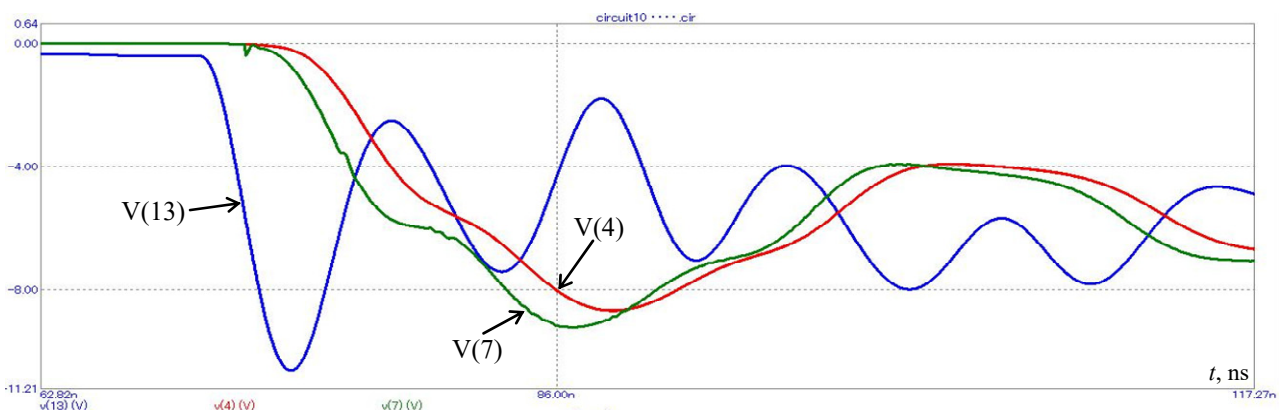


Fig. 10. Dependences of voltages $V(4)$, $V(7)$, $V(13)$ on time according to the scheme in Fig. 1. This is the case with one processing unit and increased capacity $C4$ of the water layer $C4 = 50 \text{ pF}$: initial segments of these pulses ($T = 72 \text{ ns}$, $C4 = 50 \text{ pF}$, other values as in Fig. 5.)

To illustrate the effect of the capacitance C4 of the water layer on the voltage amplitude at the processing unit, the results of simulation were taken without taking into account the delay time of the discharge in the spark gap SW2, since it is this simulation option that was considered in our work [13]. When taking into account the delay time of the discharge in the spark gap SW2 (delay in the operation of the spark gap SW2), an increase in the capacitance C4 of the water layer also leads to a decrease in the voltage amplitude at the processing unit, although the effect of this increase is reduced.

Conclusions. To increase the voltage amplitude at the processing node and on the water layer in this node, it is necessary to reduce the load capacitance (capacity of the water layer in the processing node) to 10 pF or less, increase the active resistance of the water layer to 500 Ω or more. The maximum step in computer simulation of the process of discharging a generator of high-voltage nanosecond pulses to an RLC load with a discharge gap should not exceed 0.01 ns. The most rational delay time for the operation of the discharger, which is the gap in the gas bubble inside the water, under the conditions considered by us is 4–5 ns. It is at this delay time that the amplitude of voltage pulses at the node of disinfecting water treatment and at the layer of treated water is maximum, other things being equal. This amplitude of voltage pulses exceeds by about 1.35 times the voltage amplitude immediately after the main high-voltage discharger, which commutates energy from the high-voltage capacitive storage to the processing node through long line filled with water.

Conflict of interest. The authors declare that they have no conflicts of interest.

REFERENCES

1. Ning W., Lai J., Kruszelnicki J., Foster J.E., Dai D., Kushner M.J. Propagation of positive discharges in an air bubble having an embedded water droplet. *Plasma Sources Science and Technology*, 2021, vol. 30, no. 1, art. no. 015005. doi: <https://doi.org/10.1088/1361-6595/abc830>.
2. Ghernaout D., Elboughdiri N. Disinfecting Water: Plasma Discharge for Removing Coronaviruses. *OALib*, 2020, vol. 7, no. 4, pp. 1-29. doi: <https://doi.org/10.4236/oalib.1106314>.
3. Gershman S. *Pulsed electrical discharge in gas bubbles in water*. Dissertation submitted for the Degree of Doctor of Philosophy, New Brunswick, New Jersey, 2008. 186 p. doi: <https://doi.org/doi:10.7282/T30Z73K8>.
4. Akkouchi K., Rahmani L., Lebid R. New application of artificial neural network-based direct power control for permanent magnet synchronous generator. *Electrical Engineering & Electromechanics*, 2021, no. 6, pp. 18-24. doi: <https://doi.org/10.20998/2074-272X.2021.6.03>.
5. Kuznetsov B.I., Nikitina T.B., Bovdvi I.V., Kolomiets V.V., Kobylanskiy B.B. Overhead power lines magnetic field reducing in multi-story building by active shielding means. *Electrical Engineering & Electromechanics*, 2021, no. 2, pp. 23-29. doi: <https://doi.org/10.20998/2074-272X.2021.2.04>.
6. Takahashi M., Shirai Y., Sugawa S. Free-Radical Generation from Bulk Nanobubbles in Aqueous Electrolyte Solutions: ESR Spin-Trap Observation of Microbubble-Treated Water. *Langmuir*, 2021, vol. 37, no. 16, pp. 5005-5011. doi: <https://doi.org/10.1021/acs.langmuir.1c00469>.
7. Nishiyama H., Nagai R., Takana H. Characterization of a Multiple Bubble Jet With a Streamer Discharge. *IEEE Transactions on Plasma Science*, 2011, vol. 39, no. 11, pp. 2660-2661. doi: <https://doi.org/10.1109/TPS.2011.2160367>.
8. Shibata T., Nishiyama H. Water Treatment by Dielectric Barrier Discharge Tube with Vapor Flow. *International Journal of Plasma Environmental Science and Technology*. 2017, vol. 11, no. 1, pp. 112-117. doi: <https://doi.org/10.34343/ijpest.2017.11.01.112>.
9. Hong J., Zhang T., Zhou R., Zhou R., Ostikov K., Rezaeimotlagh A., Cullen P.J. Plasma bubbles: a route to sustainable chemistry. *AAPPS Bulletin*, 2021, vol. 31, no. 1, art. no. 26. doi: <https://doi.org/10.1007/s43673-021-00027-y>.
10. HyoungSup K. *Plasma Discharges in Produced Water and Its Applications to Large Scale Flow*. A Thesis Submitted to the Faculty of Drexel University for the degree of Doctor of Philosophy, March 2016. 205 p.
11. Takahashi K., Takayama H., Kobayashi S., Takeda M., Nagata Y., Karashima K., Takaki K., Namihira T. Observation of the development of pulsed discharge inside a bubble under water using ICCD cameras. *Vacuum*, 2020, vol. 182, art. no. 109690. doi: <https://doi.org/10.1016/j.vacuum.2020.109690>.
12. Sponsel N.L., Gershman S., Herrera Quesada M.J., Mast J.T., Stapelmann K. Electric discharge initiation in water with gas bubbles: A time scale approach. *Journal of Vacuum Science & Technology A*, 2022, vol. 40, no. 6, art. no. 063002. doi: <https://doi.org/10.1116/6.0001990>.
13. Boyko M.I., Makogon A.V. Discharge in gas bubbles in water as a source of an intensive factors' complex for water disinfection: comparison experimental and computer modelling results. *Technical Electrodynamics*, 2022, no. 3, pp. 56-61. doi: <https://doi.org/10.15407/techned2022.03.056>.
14. Boyko N.I., Makogon A.V. High voltage plant with 3 MW pulse power for disinfection flow of water by nanosecond discharges in gas bubbles. *Technical Electrodynamics*, 2020, no. 5, pp. 80-83. doi: <https://doi.org/10.15407/techned2020.05.080>.
15. Mesiats G.A. *Generation of power nanosecond pulses*. Moscow, Soviet Radio Publ., 1974. 256 p. (Rus).

Received 23.03.2023

Accepted 30.05.2023

Published 02.01.2024

M.I. Boiko¹, Doctor of Technical Sciences, Professor,
K.S. Tatkova¹, Master Student,
¹National Technical University «Kharkiv Polytechnic Institute»,
2, Kyrpychova Str., Kharkiv, 61002, Ukraine,
e-mail: qnaboyg@gmail.com (Corresponding Author)

How to cite this article:

Boiko M.I., Tatkova K.S. Computer simulation of operation plant effective modes for water disinfection by electrical discharges in gas bubbles. *Electrical Engineering & Electromechanics*, 2024, no. 1, pp. 43-50. doi: <https://doi.org/10.20998/2074-272X.2024.1.06>